Applied Ocean Research 118 (2022) 102927

Contents lists available at ScienceDirect

Applied Ocean Research

journal homepage: www.elsevier.com/locate/apor

Short-term ship motion attitude prediction based on LSTM and GPR

Qian Sun [a,b], Zhong Tang [a,b], Jingpeng Gao [a,b], Guochang Zhang [c,*]

[a] College of Information and Communication, Harbin Engineering University, Harbin, 150001, China
[b] Key Laboratory of Advanced Marine Communication and Information Technology, Ministry of Industry and Information Technology, Harbin Engineering University, Harbin, 150001, China
[c] College of Shipbuilding Engineering, Harbin Engineering University, Harbin, 150001, China

ARTICLE INFO

Keywords:
Ship motion attitude
Short-term prediction
Long Short-Term Memory Network
Gaussian Process Regression

ABSTRACT

The random motions of a ship due to the sea waves directly affects the safety and efficiency of marine operations. Accurate short-term ship attitude prediction plays a vital role in operational decision-making in future seconds. In this paper, a new hybrid prediction model of ship motion attitude is proposed based on Long Short-Term Memory (LSTM) neural network and Gaussian Process Regression (GPR). When dealing with nonlinear regression problems, LSTM model can get high-accuracy point prediction results, while GPR model with lower prediction accuracy can obtain interval prediction results with probability distribution significance. The LSTM-GPR model successfully combines the advantages of LSTM and GPR, and can obtain high-accuracy point prediction results and reliable interval prediction results at the same time. The prediction experiments of ship rolling angle and pitch angle are carried out under both motion and static conditions. The results show that the LSTM-GPR hybrid model can obtain reliable interval prediction results without reducing the forecasting accuracy of LSTM model, which verifies the effectiveness and advancement of the hybrid model.

1. Introduction

Large ships are equipped with radar, photoelectric detection, carrier-based aircrafts and other equipments. High accuracy attitude prediction is conducive to guiding these weapon equipment. Due to the random and disordered wave forces and various external factors, large ships will continuously produce six degrees of freedom random motions in the sea. These random motions directly affect the safety and efficiency of marine operations such as the take-off and landing of carrier-based aircraft on aircraft carriers (Qu et al., 2016), cargo transfer between ships (Huang et al., 2014) and ship-borne helicopter recovery (Yang, 2013), especially in harsh conditions. Improving the accuracy of ship attitude prediction is conducive to decision-making for performing motion sensitive maritime activities and obtaining reliable prediction uncertainty information is also beneficial to avoid potential navigation risks. Therefore, obtaining high accuracy ship attitude prediction results and reliable interval prediction results is of great significance to ships operating at sea.

Ship motion attitude prediction modeling is the prerequisite for achieving accurate attitude prediction which commonly can be divided into four categories, which are hydrodynamics-based model, classical time series model, artificial intelligence model and hybrid model. In hydrodynamics-based model, the wave height at a certain distance in front of the bow is taken as the input signal and convoluted with the kernel function of ship response function to predict the ship's motion attitude (Kaplan, 1969). In practical applications, it is difficult to obtain high-precision input signals and ship response functions, resulting in low prediction accuracy, which limits the application of this model.

The time series model based method uses the historical data of the ship motion attitude to establish a forecast model, which can avoid solving the response function and state equations of the ship (Yumori, 1981). Time series models mainly include Auto-regressive model (AR), Auto-regressive Moving Average model (ARMA) and their variants. Among these models, AR model is widely used because of its low computational time consumption and high adaptability (Jiang et al., 2020). To further improve the prediction accuracy, Yumori proposes an improved ARMA model based on AR model (Yumori, 1981), which uses the incoming wave records as inputs in addition to the ship motion samples. The time series models have a small calculation amount and low cost, but they are not suitable for nonlinear problems under complex sea conditions such as ship motion attitude prediction.

In order to deal with the strong non-linearity of ship motion, various artificial intelligent methods are proposed to forecast ship motion attitude, such as Artificial Neural Networks (ANN) (Khan et al., 2007), Support Vector Machine (SVM) (Zhou and Shi, 2013), Back Propagation Neural Network (BPNN) (Ge et al., 2017) and Radial Basis Function

* Corresponding author.
E-mail address: zhangguochang2020@163.com (G. Zhang).

https://doi.org/10.1016/j.apor.2021.102927
Received 3 January 2021; Received in revised form 15 September 2021; Accepted 12 October 2021
Available online 8 November 2021

(RBF) network (Yin et al., 2018). In recent years, Recurrent Neural Network (RNN) has received extensive attention because of its excellent performance in time series prediction. It was extensively explored to solve various nonlinear time series problems such as stock market prediction (Akita et al., 2016), wave height prediction (Ni and Ma, 2020), traffic flow forecasting (Chen et al., 2016), and wind speed forecasting (Zhang et al., 2019), etc. However, the original RNN model suffers gradient explosion and vanish in the process of long sequence training. Long Short-Term Memory (LSTM) network is proposed to solve this problem by adding input gates, output gates and forget gates to the RNN (Gers et al., 2000). LSTM deep learning model provides a potential way for nonlinear ship motions prediction due to its capability in non-linearity processing (Liu et al., 2020). Although the artificial intelligence models perform well in time series prediction, there are still some problems in practical applications due to the poor adaptability of the models and the strong randomness of the ship motion attitude, such as a single forecast result and unsatisfactory forecast accuracy (Ge et al., 2017; Wang et al., 2017). Therefore, a variety of hybrid prediction models have been proposed by many researchers.

The hybrid prediction method is the hot spot of the current forecasting research. Nie et al. applied empirical mode decomposition (EMD) and mirror symmetry to SVM model (Nie et al., 2020), which confirms the negative EMD boundary effect on the prediction accuracy of classical EMD-SVR model and validity of the mirror symmetry method using the rolling and pitching of ship motion data collected during sailing for experiments. An EMD based least square support vector machines (LSSVM) is proposed for ship motion prediction, which improves the prediction accuracy of the coming 10 s (Zhou and Shi, 2013). And many other scholars also applied the combined forecasting method to ship motion prediction problems (Gu et al., 2013; Zhang et al., 2020; Bian et al., 2016). Compared with the single prediction method, the hybrid method has better performance in forecast accuracy.

The above studies focus on the accuracy of ship motion attitude prediction and seldom consider the uncertainty of the prediction results. The prediction accuracy is indeed an important index in the research of ship motion attitude prediction, but obtaining reliable prediction uncertainty information is also conducive to improving the safety and efficiency of marine operations. At present, Gaussian process regression (GPR) method has been successfully applied to time series prediction in some fields. For example, the hybrid model of probabilistic wind speed prediction based on AR model and GPR can not only improve the accuracy of point forecast, but also generate satisfactory prediction intervals (Zhang et al., 2016). In this paper, a new hybrid prediction model based on LSTM neural network and GPR is proposed, which adopts the idea of two-step prediction. Firstly, the LSTM network is trained completely, then the training set and test set are used as inputs to make the first prediction with LSTM. After that, GPR is constructed between the first prediction value and the observed value for the second prediction. The results of the second prediction include point prediction, interval prediction and probability prediction. In this study, our proposed LSTM-GPR prediction model does not require the time series to conform to a strict Gaussian distribution. As long as the appropriate kernel function is set, the data with different characteristics can be modeled and forecasted. The first advantage of this hybrid model is that the final point prediction results do not reduce the prediction accuracy of LSTM. Because of the high accuracy point prediction of LSTM, establishing GPR model between the first prediction value and the observed value can obtain more reliable prediction interval, which is the second advantage of the hybrid model. The LSTM-GPR hybrid prediction model can obtain reliable interval prediction results without reducing ship motion attitude prediction accuracy of LSTM model.

The rest of the paper is organized as follows. In Section 2, the implementation details of the LSTM-GPR model are introduced. Section 3 describes the preparations for the experiments. In Section 4, the LSTM-GPR model is applied to the experimental data collected from a real ship. Finally, Section 5 summarizes the work of this paper and gives the conclusions.

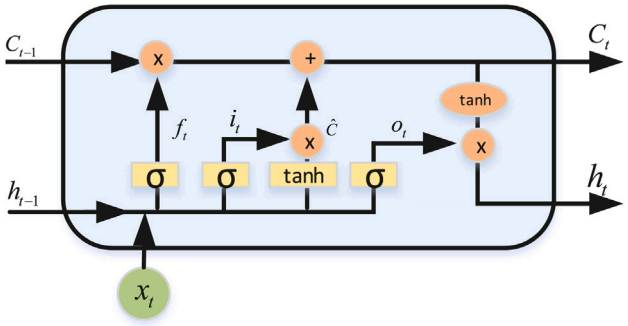

Fig. 1. LSTM cell structure.

2. Methodology

2.1. Long short term memory network (LSTM)

LSTM, a special Recurrent Neural Network (RNN), is mainly used to solve the problems of gradient vanishing and gradient explosion in the process of long sequence training. Compared with ordinary RNN, LSTM has better performance in time series prediction. The core of LSTM is the cell state, which is the main information in the process of data transmission. LSTM network can delete or add information to cell state through a structure called gate. The LSTM cell contains three gates to control the cell state, which are forget gate, input gate and output gate. The LSTM cell structure is shown in Fig. 1.

In Fig. 1, C_t, C_{t-1} and $\hat{C}_t$ represent the current cell state, the previous cell state and the temporary state, respectively. In the process of data transmission, the information of each step C_t does not completely copy the previous step C_{t-1}, but chooses to forget some content and remember some new content on the basis of C_{t-1}. x_t denotes the present input, h_t and h_{t-1} respectively represent the current hidden state and the previous hidden state. Forget gate f_t, input gate i_t and output gate o_t respectively determine the information which will be discarded from the previous cell, the information which will be added to the current cell and the information which will be exported from the current cell. They are given in Eqs. (1)–(3):

$$f_t = \sigma\left(W_f \cdot \left[h_{t-1}, x_t\right] + b_f\right) \tag{1}$$

$$i_t = \sigma\left(W_i \cdot \left[h_{t-1}, x_t\right] + b_i\right) \tag{2}$$

$$o_t = \sigma\left(W_o \cdot \left[h_{t-1}, x_t\right] + b_o\right) \tag{3}$$

For LSTM cell state, it is expressed as follows:

$$C_t = f_t * C_{t-1} + i_t * \hat{C}_t \tag{4}$$

$$\hat{C}_t = \tanh\left(W_C \cdot \left[h_{t-1}, x_t\right] + b_C\right) \tag{5}$$

For LSTM cell hidden state h_t, it is expressed as follows:

$$h_t = o_t * \tanh(C_t) \tag{6}$$

where W_f, W_i and W_o represent the weight matrix of forget gate, input gate and output gate, respectively. Similarly, b_f, b_i and b_o represent the offset vector of forget gate, input gate and output gate, respectively. In addition, W_C and b_C denote the weight matrix and offset vector of the current cell state, σ and tanh are the activation functions, their calculation formulas are as follows:

$$\sigma(x) = \frac{1}{1 + e^{-x}} \tag{7}$$

$$\tanh(x) = \frac{e^{x} - e^{-x}}{e^{x} + e^{-x}} \tag{8}$$

Like all neural network models, the initialization parameters of the LSTM neural network are randomly generated. It uses the training data

set to calculate the loss function, and based on the Back Propagation Through Time (BPTT) algorithm to reverse solve the gradient, and then adjust the model parameters according to the gradient until convergence. The processes and formulas of error back propagation in the tth period are derived as follows:

First, the most common squared error function is used as the loss function to be optimized:

$$E_t = \frac{1}{2}\left(y_t - Y_t\right)^2 \tag{9}$$

where E_t denotes the error in the tth period. y_t and Y_t are predictions and observations in the tth period, respectively. In back propagation, the weight matrix W_f, W_i, W_o and W_C are divided into two parts W_{fh}, W_{fx}, W_{ih}, W_{ix}, W_{oh}, W_{ox}, W_{Ch} and W_{Cx}. LSTM has four weighted inputs corresponding to f_t, i_t, o_t and C_t, respectively. We define these four weighted inputs and their corresponding error terms as follows:

$$\mathbf{net}_{f,t} = W_f\left[\mathbf{h}_{t-1}, \mathbf{x}_t\right] + \mathbf{b}_f = W_{fh}\mathbf{h}_{t-1} + W_{fx}\mathbf{x}_t + \mathbf{b}_f \tag{10}$$

$$\mathbf{net}_{i,t} = W_i\left[\mathbf{h}_{t-1}, \mathbf{x}_t\right] + \mathbf{b}_i = W_{ih}\mathbf{h}_{t-1} + W_{ix}\mathbf{x}_t + \mathbf{b}_i \tag{11}$$

$$\mathbf{net}_{o,t} = W_o\left[\mathbf{h}_{t-1}, \mathbf{x}_t\right] + \mathbf{b}_o = W_{oh}\mathbf{h}_{t-1} + W_{ox}\mathbf{x}_t + \mathbf{b}_o \tag{12}$$

$$\mathbf{net}_{\hat{C},t} = W_C\left[\mathbf{h}_{t-1}, \mathbf{x}_t\right] + \mathbf{b}_C = W_{Ch}\mathbf{h}_{t-1} + W_{Cx}\mathbf{x}_t + \mathbf{b}_C \tag{13}$$

$$\delta_{f,t} \overset{def}{=} \frac{\partial E_t}{\partial \mathbf{net}_{f,t}} \tag{14}$$

$$\delta_{i,t} \overset{\text{def}}{=} \frac{\partial E_t}{\partial \mathbf{net}_{i,t}} \tag{15}$$

$$\delta_{o,t} \overset{\text{def}}{=} \frac{\partial E_t}{\partial \mathbf{net}_{o,t}} \tag{16}$$

$$\delta_{\hat{C},t} \overset{\text{def}}{=} \frac{\partial E_t}{\partial \mathbf{net}_{\hat{C},t}} \tag{17}$$

To pass the error term backward along time is to calculate the error term δ_{t-1}^T at $t-1$ period.

$$\begin{aligned}\delta_{t-1}^T &= \frac{\partial E_t}{\partial \mathbf{h}_{t-1}} = \frac{\partial E_t}{\partial \mathbf{h}_t}\frac{\partial \mathbf{h}_t}{\partial \mathbf{h}_{t-1}} = \delta_t^T \frac{\partial \mathbf{h}_t}{\partial \mathbf{h}_{t-1}} \\ &= \delta_{o,t}^T \frac{\partial \mathbf{net}_{o,t}}{\partial \mathbf{h}_{t-1}} + \delta_{f,t}^T \frac{\partial \mathbf{net}_{f,t}}{\partial \mathbf{h}_{t-1}} + \delta_{i,t}^T \frac{\partial \mathbf{net}_{i,t}}{\partial \mathbf{h}_{t-1}} + \delta_{\hat{C},t}^T \frac{\partial \mathbf{net}_{\hat{C},t}}{\partial \mathbf{h}_{t-1}} \\ &= \delta_{o,t}^T W_{oh} + \delta_{f,t}^T W_{fh} + \delta_{i,t}^T W_{ih} + \delta_{\hat{C},t}^T W_{Ch}\end{aligned} \tag{18}$$

According to the definition of $\delta_{f,t}$, $\delta_{i,t}$, $\delta_{o,t}$ and $\delta_{\tilde{C},t}$, we can derive the following formulae:

$$\delta_{f,t}^T = \delta_t^T * \mathbf{o}_t * \left(1 - \tanh\left(C_t\right)^2\right) * C_{t-1} * f_t * \left(1 - f_t\right) \tag{19}$$

$$\delta_{i,t}^T = \delta_t^T * \mathbf{o}_t * \left(1 - \tanh\left(C_t\right)^2\right) * \hat{C}_t * \mathbf{i}_t * \left(1 - \mathbf{i}_t\right) \tag{20}$$

$$\delta_{o,t}^T = \delta_t^T * \tanh\left(C_t\right) * \mathbf{o}_t * \left(\mathbf{1} - \mathbf{o}_t\right) \tag{21}$$

$$\delta_{\hat{C},t}^T = \delta_t^T * \mathbf{o}_t * \left(1 - \tanh\left(C_t\right)^2\right) * \mathbf{i}_t * \left(1 - \hat{C}^2\right) \tag{22}$$

Eqs. (18)–(22) represent the process of propagating the error back for a moment along time. Now, we can get the formula to pass the error term forward to any k moment.

$$\delta_k^T = \prod_{j=k}^{t-1} \delta_{o,j}^T W_{oh} + \delta_{f,j}^T W_{fh} + \delta_{i,j}^T W_{ih} + \delta_{\hat{C},j}^T W_{Ch} \tag{23}$$

For the weight gradient of W_{fh}, W_{ih}, W_{oh}, W_{Ch}, b_f, b_i, b_o, and b_C, we first calculate their gradients at t moment $\frac{\partial E_t}{\partial W_{oh,t}}$, and then add up the gradients at each time to get the final gradient $\frac{\partial E_t}{\partial W_{oh}}$. Take W_{fh} as an example, the calculation details are as follows:

$$\frac{\partial E_t}{\partial W_{oh,t}} = \frac{\partial E_t}{\partial \mathbf{net}_{o,t}}\frac{\partial \mathbf{net}_{o,t}}{\partial W_{oh,t}} = \delta_{o,t}\mathbf{h}_{t-1}^T \tag{24}$$

$$\frac{\partial E_t}{\partial W_{oh}} = \sum_{j=1}^{t} \delta_{o,j}\mathbf{h}_{j-1}^T \tag{25}$$

For the weight gradient of W_{fx}, W_{ix}, W_{ox}, W_{Cx}, they can be calculated directly according to the corresponding error term. Take W_{fx} as an example, the calculation details are as follows:

$$\frac{\partial E_t}{\partial W_{ox}} = \frac{\partial E_t}{\partial \mathbf{net}_{o,t}}\frac{\partial \mathbf{net}_{o,t}}{\partial W_{ox}} = \delta_{o,t}\mathbf{x}_t^T \tag{26}$$

Through the above formulas, the training algorithm in deep learning can be used to optimize the weights to minimize the loss function.

2.2. Gaussian process regression (GPR)

Gaussian process regression is a data-driven method. It is suitable for nonlinear and multi-dimensional regression problems, and can show the confidence interval of prediction results. The Gaussian process is defined as (Rasmussen, 2003):

$$f(\mathbf{x}) \sim \mathcal{GP}\left(m(x), k\left(x, x'\right)\right) \tag{27}$$

where $m(x)$ denotes the mean function and $k\left(x, x'\right)$ is a covariance function that describes the degree of similarity or correlation between different samples. The covariance function is a key factor affecting the prediction performance of Gaussian process regression.

We assume a regression model with noise as follows:

$$Y = f(x) + \xi \tag{28}$$

where Y is observation and $f(x)$ is an underlying function. The noise ξ is assumed to be Gaussian distribution with zero mean and variance σ_n^2, $\xi \sim N\left(0, \sigma_n^2\right)$.

Because the data can be represented as a sample from a multivariate Gaussian distribution in Gaussian process modeling, we can obtain the prior distribution of the observation Y and the joint prior distribution of the observed value Y and the predicted value y.

$$Y \sim N(0, K(X, X) + \sigma_n^2 I_n) \tag{29}$$

$$\begin{aligned}\begin{bmatrix} Y \\ \mathrm{y} \end{bmatrix} &\sim N\left(0, \begin{bmatrix} K(X,X) + \sigma_n^2 I_n & K(X, X_*) \\ K(X_*, X) & K(X_*, X_*) \end{bmatrix}\right) \\ &= N\left(0, \begin{bmatrix} K & K_*^T \\ K_* & K_{**} \end{bmatrix}\right)\end{aligned} \tag{30}$$

where $K(X, X)$ is a symmetric positive definite covariance matrix. $K(X_*, X)$ and $K(X, X_*)$ are the covariance matrices between the test set X and training set X_*. $K(X_*, X_*)$ is the covariance matrix of the test set itself. I_n is an n-dimensional unit matrix. The covariance matrix $K(X, X)$ is defined as:

$$K(X,X) = \begin{bmatrix} k\left(x_1, x_1\right) & k\left(x_1, x_2\right) & \cdots & k\left(x_1, x_n\right) \\ k\left(x_2, x_1\right) & k\left(x_2, x_2\right) & \cdots & k\left(x_2, x_n\right) \\ \vdots & \vdots & \ddots & \vdots \\ k\left(x_n, x_1\right) & k\left(x_n, x_2\right) & \cdots & k\left(x_n, x_n\right) \end{bmatrix} \tag{31}$$

The squared exponential covariance function is expressed as:

$$k\left(x, x'\right) = p_1 . \exp\left(-\frac{(x - x')^2}{2p_2}\right) \tag{32}$$

where p_1 and p_2 are called hyper-parameters. p_1 denotes the amplitude that specifies the maximum allowable covariance. p_2 is the length scale parameter, which defines the rate of decay in correlation for points farther away from each other.

The posterior distribution of the predicted value y is

$$y|Y \sim N(\bar{y}, \sigma_y^2) \tag{33}$$

The mean and variance of this Gaussian distribution are expressed as

$$\bar{y} = K_* K^{-1} Y \tag{34}$$

$$\sigma_y^2 = K_{**} - K_* K^{-1} K_*^T \tag{35}$$

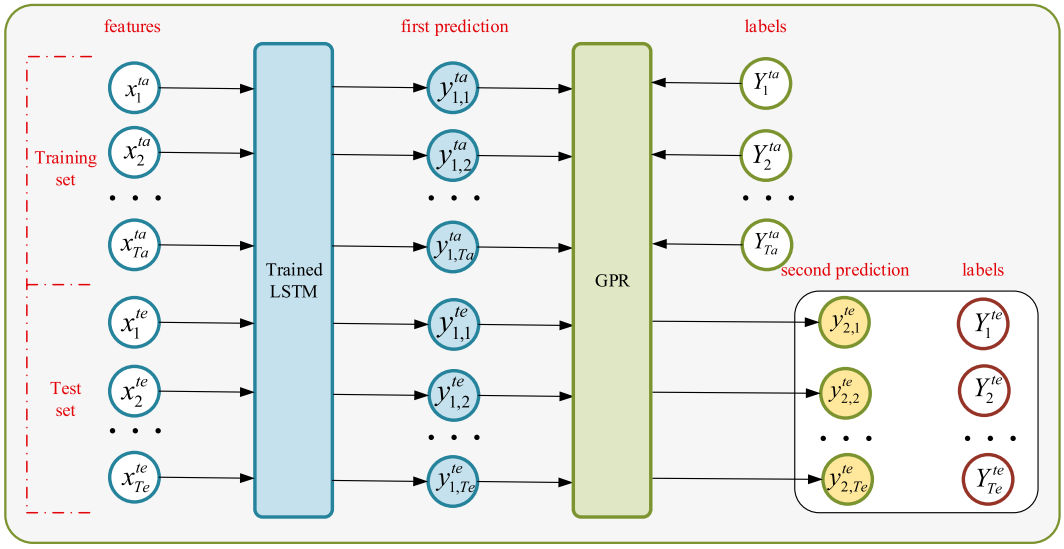

Fig. 2. Flowchart of LSTM-GPR model.

Therefore, the mean of the predictive distribution is used as the point prediction. The interval prediction can be calculated using the predictive mean and the variance. According to the property of Gaussian distribution, the interval prediction result corresponding to the 95% confidence level is $[\bar{y} - 1.96\sigma_y, \bar{y} + 1.96\sigma_y]$. The probability density function of t-th predicted value is as follows:

$$p(y_t) = \frac{1}{\sqrt{2\pi}\sigma_{yt}} \exp(-\frac{(y_t - \bar{y}_t)^2}{2\sigma_{yt}^2}) \tag{36}$$

2.3. LSTM-GPR hybrid model

For nonlinear regression problems, using LSTM neural network can get high-precision point prediction results. In contrast, the Gaussian process regression algorithm is not as accurate as the LSTM neural network when solving such problems, but the GPR model can obtain interval prediction results with probability distribution significance. This paper combines LSTM neural network and GPR to form a hybrid prediction model. The flowchart of LSTM-GPR model is shown in Fig. 2. The implementation steps of the hybrid forecasting model are as follows:

It is assumed that the original time series is represented as $F = [F_1, F_2, \ldots, F_{Ta+Te}]$. The sequence is divided into training set $F^{ta} = [F_1^{ta}, F_2^{ta}, \ldots, F_{Ta}^{ta}]$ and test set $F^{te} = [F_1^{te}, F_2^{te}, \ldots, F_{Te}^{te}]$. Ta and Te are the number of training set and test set samples. In order to find the mapping relationship between the prediction results and historical data, it is necessary to reconstruct the one-dimensional time series. The training set $D_{1st}^{ta} = [X_{1st}^{ta}, Y_{1st}^{ta}]$ and test set $D_{1st}^{te} = [X_{1st}^{te}, Y_{1st}^{te}]$ for the first prediction are expressed as follows:

$$X_{1st}^{ta} = \left[x_1^{ta}, x_2^{ta}, \ldots, x_{Ta}^{ta}\right], x_t^{ta} = \left[F_{t-1}^{ta}, F_{t-2}^{ta}, \ldots\right] \tag{37}$$

$$Y_{1st}^{ta} = \left[Y_1^{ta}, Y_2^{ta}, \ldots, Y_{Ta}^{ta}\right], Y_t^{ta} = \left[F_t^{ta}\right] \tag{38}$$

$$X_{1st}^{te} = \left[x_1^{te}, x_2^{te}, \ldots, x_{Te}^{te}\right], x_t^{te} = \left[F_{t-1}^{te}, F_{t-2}^{te}, \ldots\right] \tag{39}$$

$$Y_{1st}^{te} = \left[Y_1^{te}, Y_2^{te}, \ldots, Y_{Te}^{te}\right], Y_t^{te} = \left[F_t^{te}\right] \tag{40}$$

The obtained training set and test set are used for the training and verification of LSTM neural network model. Then, taking $[X_{1st}^{ta}, X_{1st}^{te}]$ as the input of the trained LSTM to get the first prediction result, which is expressed as $[y_{1,1}^{ta}, y_{1,2}^{ta}, \ldots, y_{1,\mathrm{Ta}}^{ta}, y_{1,1}^{te}, y_{1,2}^{te}, \ldots, y_{1,\mathrm{Te}}^{te}]$. Based on the results of the first prediction, the training set and test set are reconstructed. We use the results of the first prediction $y_{1,t}^{\mathrm{ta}}$ as input and the corresponding original set F_t^{ta} as output to form a training set to establish the GPR model. The training set $D_{2nd}^{ta} = [X_{2nd}^{ta}, Y_{2nd}^{ta}]$ and test set $D_{2nd}^{te} = [X_{2nd}^{te}, Y_{2nd}^{te}]$ for the second prediction are expressed as follows:

$$X_{2\mathrm{nd}}^{\mathrm{ta}} = \left[x_1^{\mathrm{ta}}, x_2^{\mathrm{ta}}, \ldots, x_{\mathrm{Ta}}^{\mathrm{ta}}\right], x_t^{\mathrm{ta}} = \left[y_{1,t}^{\mathrm{ta}}\right] \tag{41}$$

$$Y_{2nd}^{\mathrm{ta}} = \left[Y_1^{\mathrm{ta}}, Y_2^{\mathrm{ta}}, \ldots, Y_{\mathrm{Ta}}^{\mathrm{ta}}\right], Y_t^{\mathrm{ta}} = \left[F_t^{\mathrm{ta}}\right] \tag{42}$$

$$X_{2nd}^{te} = \left[x_1^{te}, x_2^{te}, \ldots, x_{Te}^{te}\right], x_t^{te} = \left[y_{1,t}^{te}\right] \tag{43}$$

$$Y_{2nd}^{te} = \left[Y_1^{te}, Y_2^{te}, \ldots, Y_{Te}^{te}\right], Y_t^{te} = \left[F_t^{te}\right] \tag{44}$$

Then, taking $X_{2nd}^{te} = [x_1^{te}, x_2^{te}, \ldots, x_{Te}^{te}]$ as the input of the trained GPR model to get the second prediction result, which is expressed as $[y_{2,1}^{te}, y_{2,2}^{te}, \ldots, y_{2,\mathrm{Te}}^{te}]$. This is also the final prediction result of the hybrid model. Finally, $[y_{2,1}^{te}, y_{2,2}^{te}, \ldots, y_{2,\mathrm{Te}}^{te}]$ and $Y_{2nd}^{te} = [Y_1^{te}, Y_2^{te}, \ldots, Y_{Te}^{te}]$ are used to evaluate the performance and reliability of the hybrid model.

The first advantage of this hybrid model is that the final point prediction results do not reduce the prediction accuracy of LSTM. Because of the high accuracy of LSTM point prediction, establishing GPR model between the first prediction value and the observed value can obtain more reliable interval prediction, which is the second advantage of the hybrid model.

3. Preparation for the experiment

3.1. Descriptions of the experimental data

The experimental data in this paper are all collected from a real ship, which is a large military ship. In order to verify the effectiveness of the prediction model proposed in this paper, different experiments under static state and motion state are designed, respectively. Both “static state” and “motion state” represent the state of the ship when we measure the experimental data of ship attitude. “Static state” means that the ship is docked at the port. “Motion state” means that the ship is sailing at a certain speed. The scene of raw data acquisition is shown as Fig. 3. Continuous ship motion attitude information is collected by inertial measurement unit (IMU) installed on the ship. The sampling frequency of the IMU is 4 Hz.

Fig. 4 shows the raw rolling angle and pitch angle of the ship in motion state. Fig. 5 shows the raw rolling angle and pitch angle of the ship in static state. In each set of data, a total of 1000 data points are selected from 250 s continuous ship roll angle and pitch angle data. The first 200 s are used as the training data set, and the last 50 s are used as the test data set.

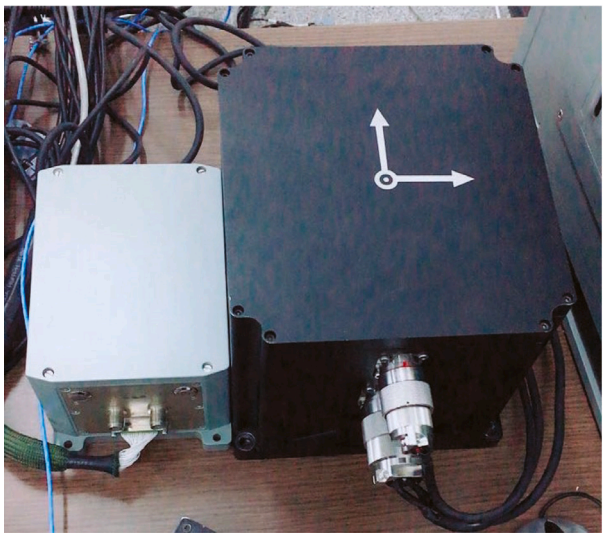

Fig. 3. The scene of raw data acquisition.

3.2. Evaluation of prediction performance

This paper mainly selects RMSE (Root Mean Square Error), MAE (Mean Absolute Errors) and MAPE (Mean Absolute Percentage Errors) as the evaluation indicators of the prediction results. The calculation formulas are as follows:

$$RMSE = \sqrt{\frac{1}{Te}\sum_{i=1}^{Te}(y_i - Y_i)^2} \tag{45}$$

$$MAE = \frac{1}{Te}\sum_{i=1}^{Te}|y_i - Y_i| \tag{46}$$

$$MAPE = \frac{1}{Te}\sum_{i=1}^{Te}\left|\frac{y_i - Y_i}{y_i}\right| \times 100\% \tag{47}$$

where y_i is the predicted value, Y_i is the observed value, and Te is the number of test set samples. RMSE is more sensitive to a large deviation between the predicted values and the actual outcomes while MAE and MAPE measure the absolute differences between predicted and actual values. The smaller the evaluation index value in the above formula, the smaller the model prediction error and the higher the prediction performance.

3.3. Models parameter setting

Ship motion attitude is time series data. GPR is a traditional machine learning algorithm for time series regression. In deep learning, LSTM is good at solving time series problems. Therefore, in order to prove the effectiveness of the LSTM-GPR hybrid prediction model proposed in this paper, LSTM model and GPR model are selected as comparison models with LSTM-GPR hybrid model. In order to ensure the fairness of the experiment, the parameters of the three models compared in this paper are as consistent as possible. The specific parameter settings are presented in Table 1.

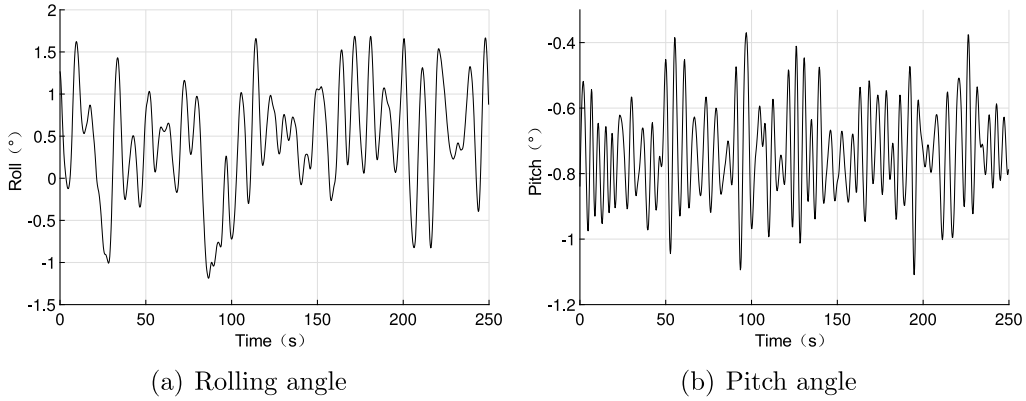

(a) Rolling angle (b) Pitch angle

Fig. 4. The raw rolling angle and pitch angle of the ship in motion state.

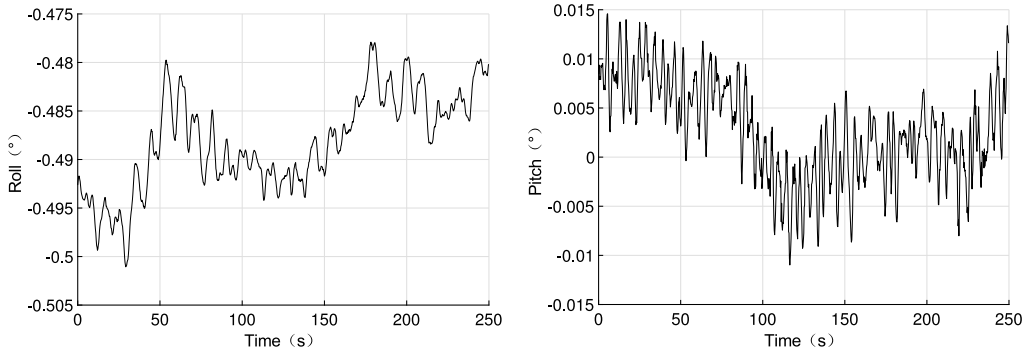

(a) Rolling angle (b) Pitch angle

Fig. 5. The raw rolling angle and pitch angle of the ship in static state.

Table 1
The specific parameter settings of models.

Model	Parameter	Meaning	Value	Reason
LSTM-GPR	n_i	Number of input layer nodes	8	Number of feature inputs
	n_h	Number of hidden layer nodes	8	Common value [2, 4, 8, 10, ...]
	n_o	Number of output layer nodes	1	Time series regression
	α	Fixed learning rate	0.01	Common value [0.01, 0.05, 0.1, ...]
	T	Size of batch	32	Common value [8, 16, 32, 50, ...]
	Ep	Epochs of training	300	Converged
	k	Kernel function	Squared exponential covariance	The same as GPR
	p_1	Parameter in kernel function	2	The same as GPR
	p_2	Parameter in kernel function	1	The same as GPR
LSTM	n_i	Number of input layer nodes	8	The same as LSTM-GPR
	n_h	Number of hidden layer nodes	8	The same as LSTM-GPR
	n_o	Number of output layer nodes	1	The same as LSTM-GPR
	α	Fixed learning rate	0.01	The same as LSTM-GPR
	T	Size of batch	32	The same as LSTM-GPR
	Ep	Epochs of training	300	The same as LSTM-GPR
GPR	k	Kernel function	Squared exponential covariance	A competitive kernel function
	p_1	Parameter in kernel function	2	Obtained from GA
	p_2	Parameter in kernel function	1	Obtained from GA

Table 2
Evaluation indexes of rolling angle prediction results (in motion state).

Model	RMSE (°)	MAE (°)	MAPE (%)
LSTM-GPR	0.0246	0.0193	5.2925
LSTM	0.0280	0.0209	6.0961
GPR	0.0355	0.0259	9.7306

Table 3
Evaluation indexes of the pitch angle prediction results (in motion state).

Model	RMSE (°)	MAE (°)	MAPE (%)
LSTM-GPR	0.0089	0.0062	0.9272
LSTM	0.0084	0.0058	0.9043
GPR	0.0103	0.0079	1.1649

Table 4
Evaluation indexes of rolling angle prediction results (in static state).

Model	RMSE (°)	MAE (°)	MAPE (%)
LSTM-GPR	0.00031	0.00023	0.0476
LSTM	0.00030	0.00025	0.0508
GPR	0.00033	0.00027	0.0568

4. Experiment of ship motion attitude prediction

4.1. Rolling angle prediction in motion state

Three prediction models have been used to predict the ship rolling angle in motion state. Fig. 6 shows the rolling angle prediction result using LSTM-GPR hybrid prediction model. Figs. 7 and 8 are the rolling angle prediction results using the LSTM model and GPR model, respectively. Figs. 6 and 8 contain not only the comparison results between the predicted rolling angle curve and the actual rolling angle curve, but also the interval prediction of rolling angle.

It is obvious from Table 2 that the error of the hybrid prediction model is lower than LSTM model and GPR model. In addition, the evaluation index value of GPR model is the highest among the three models, which indicates that LSTM performs better than GPR in prediction accuracy when predicts the rolling angle in motion state. It is known from the results that the hybrid prediction model proposed in this paper does not reduce the accuracy due to the combination of GPR, but improves the final prediction accuracy to a certain extent. It can be seen from Fig. 6, Figs. 7 and 8 that the three prediction models have strong fitting ability, and the hybrid prediction model also has the ability of interval prediction because of the combination of GPR. When predicting the rolling angle of a ship in motion state, the experimental result has reached the expectation of designing the hybrid prediction model, and verified the effectiveness and the advancement of LSTM-GPR hybrid model.

4.2. Pitch angle prediction in motion state

Three prediction models have been used to predict the ship pitch angle in motion state. Fig. 9 shows the pitch angle prediction result by using LSTM-GPR hybrid prediction model. Figs. 10 and 11 are the pitch angle prediction results using the LSTM model and GPR model respectively. Figs. 9 and 11 contain not only the comparison results between the predicted pitch angle curve and the actual pitch angle curve, but also the interval prediction of pitch angle. Table 3 shows the three evaluation index values of the prediction results of the three models.

Different from the rolling angle prediction, the evaluation index values of LSTM model are the smallest in Table 3. It indicates that LSTM model has the highest point prediction accuracy when predicting the pitch angle in motion state. Specifically, the evaluation index values of the LSTM-GPR hybrid model are slightly higher than those of LSTM model, and are greatly reduced compared with GPR model. Although LSTM model has high prediction accuracy, it is not able to predict the interval of ship pitch angle attitude. However, the hybrid model can obtain the point prediction interval without significantly reducing the prediction accuracy of LSTM model. It can be seen from Fig. 9, Fig. 10 and Fig. 11 respectively that the three prediction models have strong fitting ability, and the hybrid prediction model also has the ability of interval prediction because of the combination of GPR. When predicting the pitch angle of a ship in motion state, the experimental result has reached the expectation of designing the hybrid prediction model, and verified the effectiveness and the advancement of LSTM-GPR hybrid model.

4.3. Rolling angle prediction in static state

Three prediction models have been used to predict the ship rolling angle in static state. Fig. 12 shows the rolling angle prediction result using LSTM-GPR hybrid prediction model. Fig. 13 and Fig. 14 are the rolling angle prediction results using the LSTM model and GPR model respectively. Figs. 12 and 14 contain not only the comparison results between the predicted rolling angle curve and the actual rolling angle curve, but also the interval prediction of rolling angle. Table 4 shows the three evaluation index values of the prediction results of the three models.

It is obvious from Table 4 that the evaluation index values of GPR model are the highest, which indicates that its prediction performance

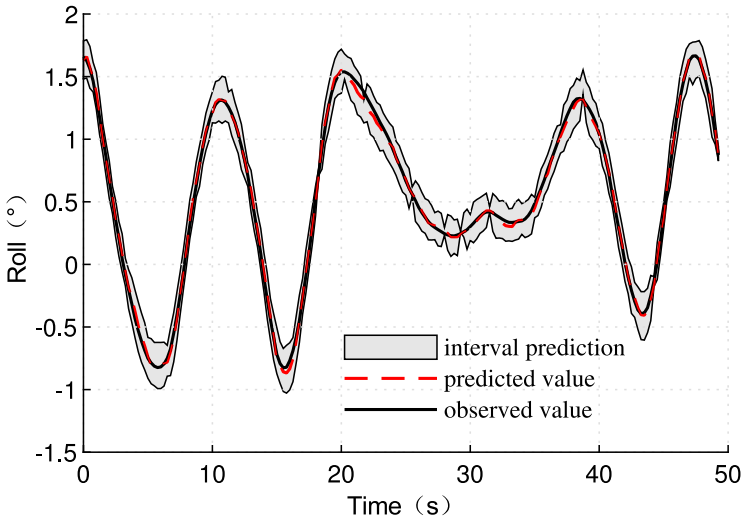

Fig. 6. Rolling angle prediction result based on LSTM-GPR hybrid model (in motion state).

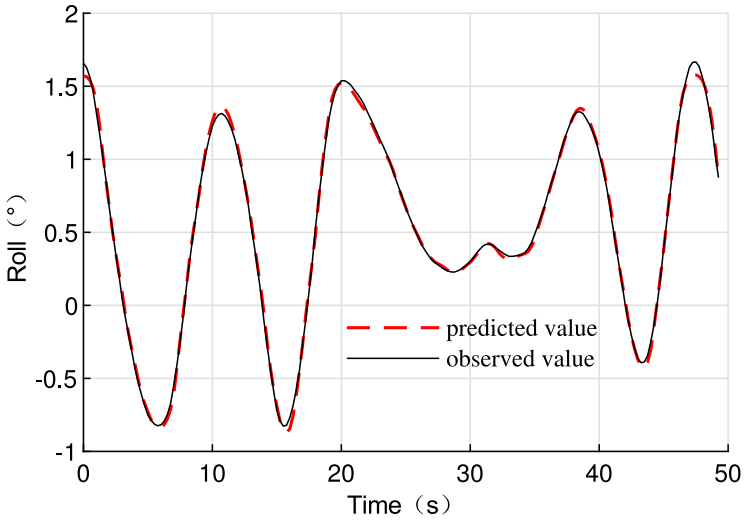

Fig. 7. Rolling angle prediction result based on LSTM model (in motion state).

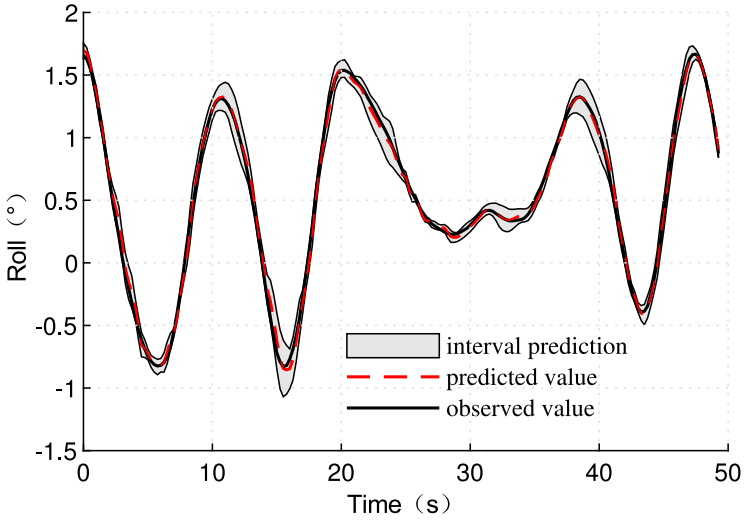

Fig. 8. Rolling angle prediction result based on GPR model (in motion state).

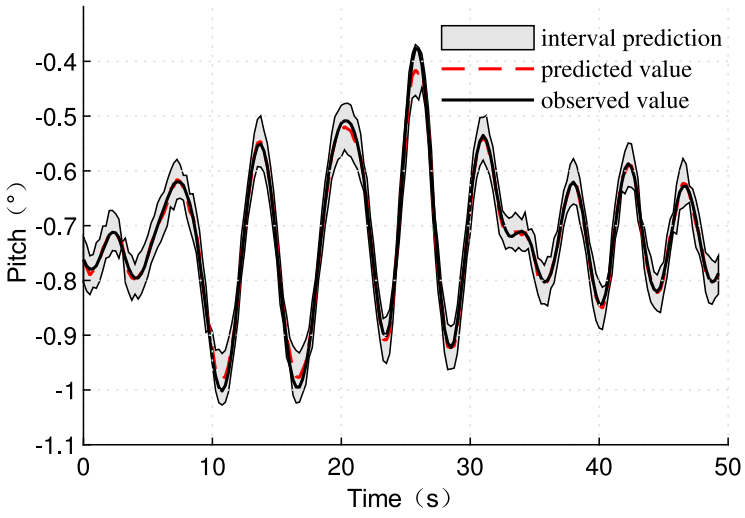

Fig. 9. Pitch angle prediction result based on LSTM-GPR hybrid model (in motion state).

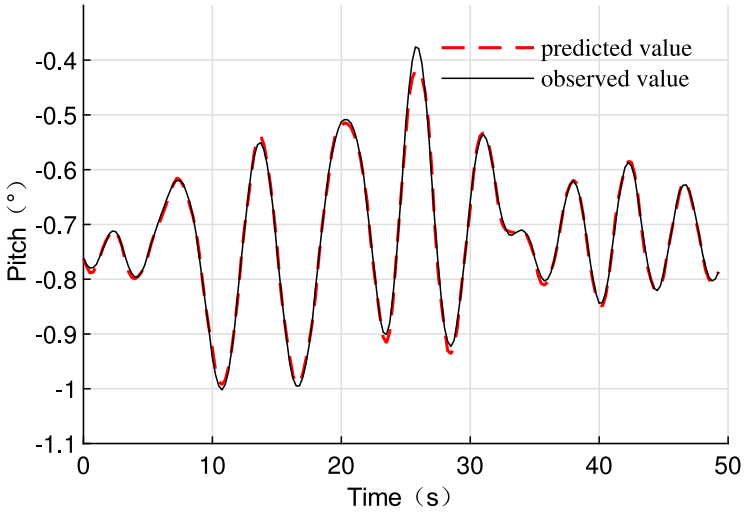

Fig. 10. Pitch angle prediction result based on LSTM model (in motion state).

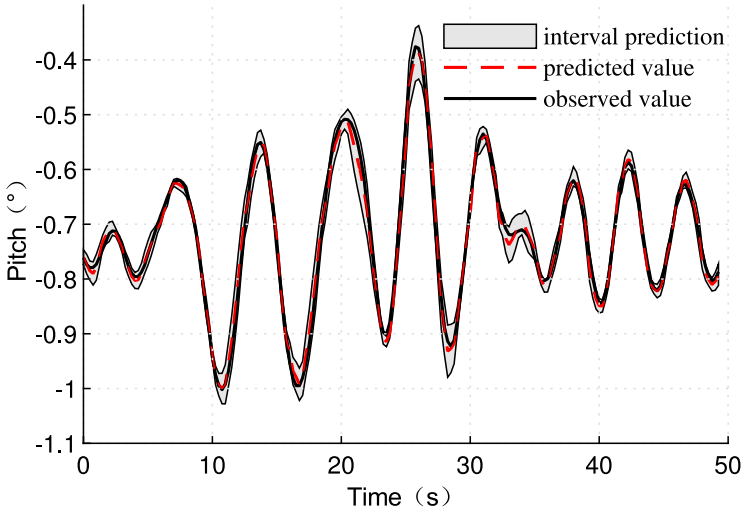

Fig. 11. Pitch angle prediction result based on GPR model (in motion state).

is the worst. The RMSE value of LSTM-GPR is higher than that of LSTM model, but the MAE value and MAPE value of LSTM-GPR are lower than those of LSTM, and the difference is very small, which indicates that the prediction accuracy of LSTM and LSTM-GPR is very close,

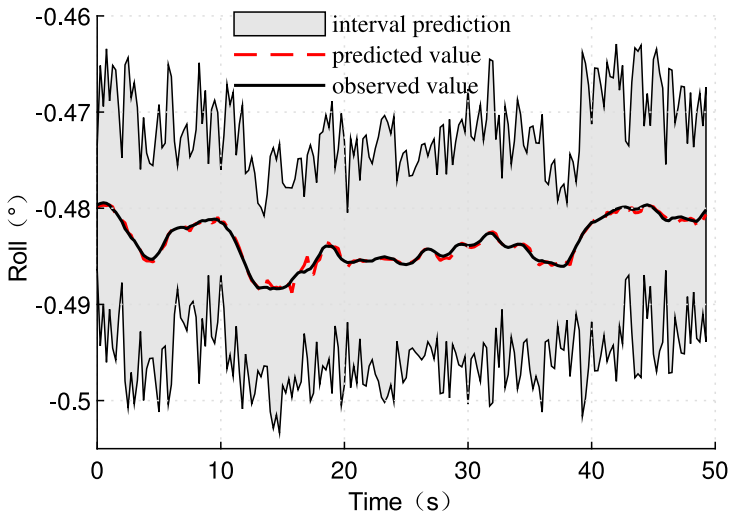

Fig. 12. Rolling angle prediction result based on LSTM-GPR hybrid model (in static state). (For interpretation of the references to colour in this figure legend, the reader is referred to the web version of this article.)

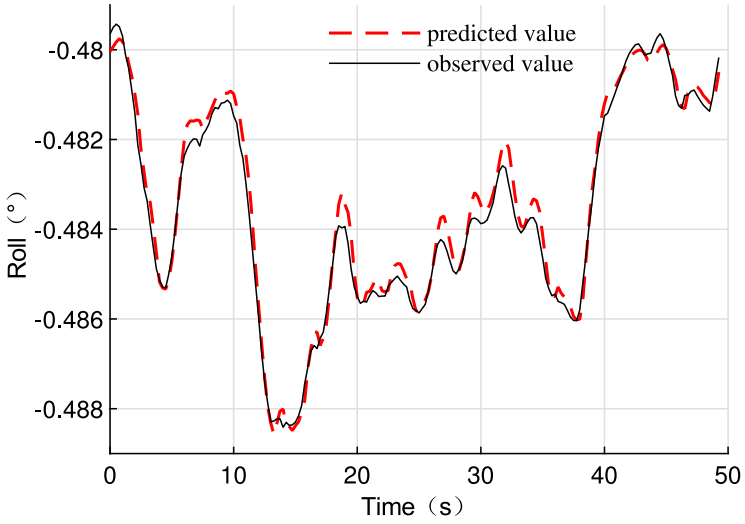

Fig. 13. Rolling angle prediction result based on LSTM model (in static state).

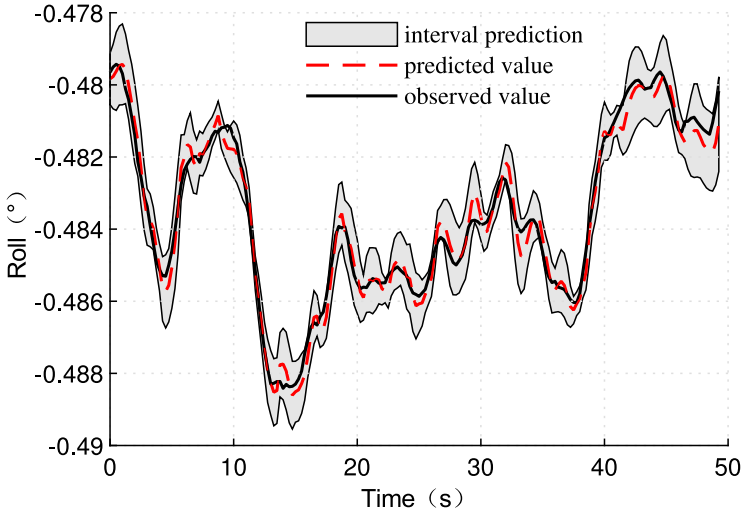

Fig. 14. Rolling angle prediction result based on GPR model (in static state). (For interpretation of the references to colour in this figure legend, the reader is referred to the web version of this article.)

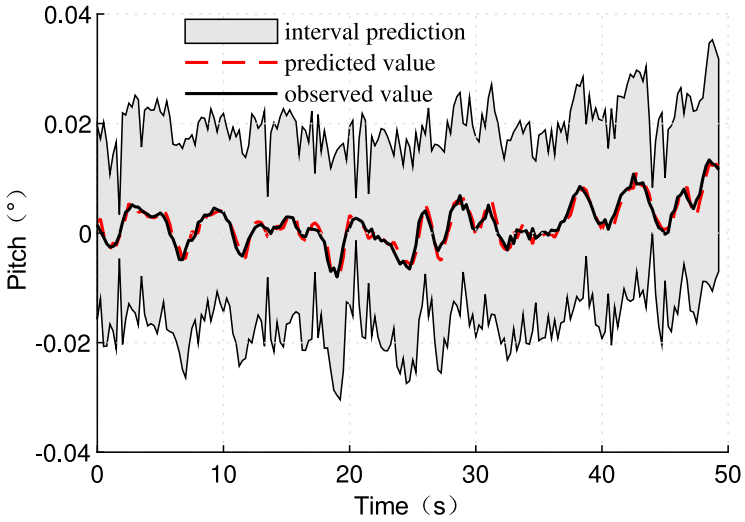

Fig. 15. Pitch angle prediction result based on LSTM-GPR hybrid model (in static state).

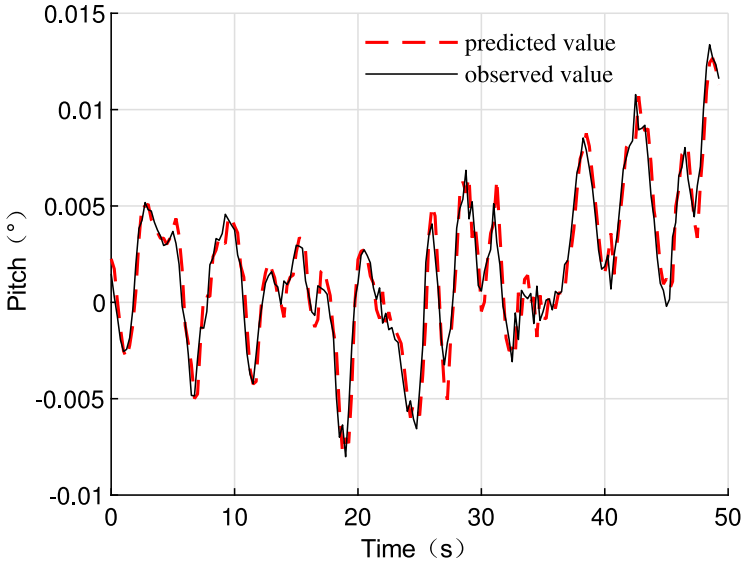

Fig. 16. Pitch angle prediction result based on LSTM model (in static state).

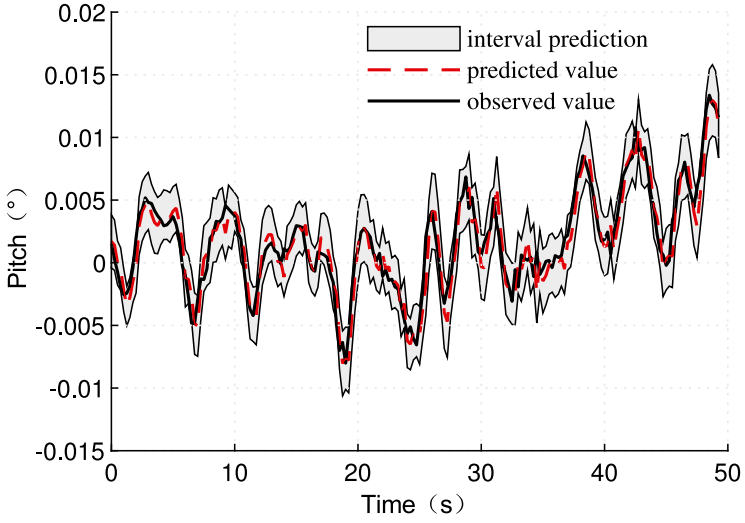

Fig. 17. Pitch angle prediction result based on GPR model (in static state).

Table 5
Evaluation indexes of the pitch angle prediction results (in static state).

Model	RMSE (°)	MAE (°)	MAPE (%)
LSTM-GPR	0.00117	0.00093	0.0930
LSTM	0.00113	0.00088	0.0883
GPR	0.00121	0.00097	0.0967

at least the prediction performance of LSTM-GPR is not worse than that of LSTM. Compared with the interval prediction results in Fig. 14, the range of interval prediction in Fig. 12 is wider. This means that the interval prediction of each time obtained by LSTM-GPR is more uncertain than that of GPR, and the red curve in the figure represents the middle value of the prediction interval. It can be seen from Fig. 5 that when the ship is in static state, the variation of rolling angle and pitch angle is very small. In this case, the two-step prediction approach of the LSTM-GPR hybrid model increases the uncertainty of the prediction results. When predicting the rolling angle of a ship in static state, although the interval prediction result of LSTM-GPR hybrid model is more uncertain than GPR model, the prediction performance is greatly improved compared with GPR model, and the problem that LSTM model does not have interval prediction is solved. Thus the experimental result has reached the expectation of designing the hybrid prediction model, and verified the effectiveness and the advancement of LSTM-GPR hybrid model.

4.4. Pitch angle prediction in static state

Three prediction models have been used to predict the ship pitch angle in static state. Fig. 15 shows the pitch angle prediction result using LSTM-GPR hybrid prediction model. Fig. 16 and Fig. 17 are the pitch angle prediction results using the LSTM model and GPR model respectively. Figs. 15 and 17 contain not only the comparison results between the predicted pitch angle curve and the actual pitch angle curve, but also the interval prediction of pitch angle. Table 5 shows the three evaluation index values of the prediction results of the three models.

Like predicting the pitch angle in motion state, the evaluation index values of LSTM model are the smallest in Table 5, which indicates that LSTM model has the highest point prediction accuracy when predicts the pitch angle in static state. The differences between the interval prediction results in Figs. 15 and 17 are similar to those shown in Figs. 12 and 14, which are determined by the characteristics of the experimental data itself. Although it is hoped that the uncertainty of predicted interval is not too large, the interval prediction result in Fig. 15 is still conducive to mastering the short-term motion attitude of a ship in the future. The LSTM-GPR hybrid model improves the prediction accuracy of GPR by combining LSTM. When predicting the pitch angle of a ship in static state, the experimental result has reached the expectation of designing the hybrid prediction model, and verified the effectiveness and the advancement of LSTM-GPR hybrid model.

The above four sets of experiments include the prediction of ship rolling angle and pitch angle under dynamic and static conditions. From the prediction results of the three models, it can be seen that the LSTM-GPR hybrid model proposed in this paper effectively combines the advantages of the high prediction accuracy of the LSTM model and the interval prediction of the GPR model. The experimental results successfully verified the effectiveness and advancement of the LSTM-GPR hybrid model. The results show that the LSTM-GPR hybrid model has a good prediction performance for the ship motion data set, but its predictive effect under different levels of sea conditions needs further verification.

5. Conclusions

Accurate short-term motion attitude prediction of large ships plays an essential role in decision making related to ship-borne maritime operations. In this paper, a new hybrid prediction model based on LSTM neural network and GPR is proposed, called LSTM-GPR model, which adopts the idea of two-step prediction. The LSTM-GPR model establishes GPR model between the predicted value by LSTM model and the observed value, which can obtain more reliable interval prediction without reducing the point prediction accuracy of LSTM model.

In order to verify that the prediction model proposed in this paper is effective for the prediction of ship attitude information in static state and in motion state, the rolling angle and pitch angle in two scenarios are selected for experiments. The results show that the LSTM-GPR hybrid model proposed in this paper effectively combines the advantages of the high prediction accuracy of the LSTM model and the interval prediction ability of the GPR model, and successfully verified the effectiveness and advancement of the LSTM-GPR hybrid model.

CRediT authorship contribution statement

Qian Sun: Formal analysis, Mathematical check, Writing – review & editing. **Zhong Tang:** Conceptualization, Methodology, Software, Writing – original draft. **Jingpeng Gao:** Validation. **Guochang Zhang:** Supervision.

Declaration of competing interest

The authors declare that they have no known competing financial interests or personal relationships that could have appeared to influence the work reported in this paper.

Acknowledgments

The paper was funded by the Fundamental Research Funds for the Central Universities (3072020CF0806), the National Natural Science Foundation of China (grant no. 51809056), and the Natural Science Foundation of Heilongjiang Province, China (grant no. F2017004).

References

Akita, R., Yoshihara, A., Matsubara, T., Uehara, K., 2016. Deep learning for stock prediction using numerical and textual information. In: 2016 IEEE/ACIS 15th International Conference on Computer and Information Science. ICIS, IEEE, pp. 1–6.

Bian, D.J., Qin, S.Q., Wu, W., 2016. A hybrid ar-dwt-emd model for the short-term prediction of nonlinear and non-stationary ship motion. In: 2016 Chinese Control and Decision Conference. CCDC, pp. 4042–4047.

Chen, Y.Y., Lv, Y., Li, Z., Wang, F., 2016. Long short-term memory model for traffic congestion prediction with online open data. In: 2016 IEEE 19th International Conference on Intelligent Transportation Systems. ITSC, pp. 132–137.

Ge, Y., Qin, M.J., Niu, Q.T., 2017. Prediction of ship motion attitude based on BP network. In: 2017 29th Chinese Control and Decision Conference. CCDC, IEEE, pp. 1596–1600.

Gers, F.A., Schmidhuber, J., Cummins, F., 2000. Learning to forget: Continual prediction with LSTM. Neural Comput. 12 (10), 2451–2471.

Gu, M., Liu, C.D., Zhang, J.F., 2013. Extreme short-term prediction of ship motion based on chaotic theory and RBF neural network. J. Ship Mech. 17 (10), 1147–1152.

Huang, L.M., Duan, W.Y., Yang, H., Chen, Y.S., 2014. A review of short-term prediction techniques for ship motions in seaway. J. Ship Mech. 18 (12), 1534–1542.

Jiang, H., Duan, S.L., Huang, L.M., Han, Y., Yang, H., Ma, Q.W., 2020. Scale effects in AR model real-time ship motion prediction. Ocean Eng. 203, 107202.

Kaplan, P., 1969. A study of prediction techniques for aircraft carrier motions at sea. J. Hydronaut. 3 (3), 121–131.

Khan, A.A., Marion, K.E., Bil, C., 2007. The prediction of ship motions and attitudes using artificial neural networks. Asor Bull. 26 (1), 2.

Liu, Y.C., Duan, W.Y., Huang, L.M., Duan, S.L., Ma, X.W., 2020. The input vector space optimization for LSTM deep learning model in real-time prediction of ship motions. Ocean Eng. 213, 107681.

Ni, C.H., Ma, X.D., 2020. An integrated long-short term memory algorithm for predicting polar westerlies wave height. Ocean Eng. 215, 107715.

Nie, Z.H., Shen, F., Xu, D.J., Li, Q.H., 2020. An EMD-SVR model for short-term prediction of ship motion using mirror symmetry and SVR algorithms to eliminate EMD boundary effect. Ocean Eng. 217, 107927.

Qu, H., Guo, R.Z., Ding, X.Z., 2016. Design of the deck longitudinal motion compensation for carrier landing. Aeronaut. Sci. Technol. 27 (12), 13–17.

Rasmussen, C.E., 2003. Gaussian processes in machine learning. In: Summer School on Machine Learning. Springer, pp. 63–71.

Wang, G.D., Han, B., Sun, W.Y., 2017. Short-term prediction of ship motion based on LSTM. Ship Sci. Technol. 39 (13), 69–72.

Yang, X.L., 2013. Displacement motion prediction of a landing deck for recovery operations of rotary UAVs. Int. J. Control Autom. Syst. 11 (1), 58–64.

Yin, J.C., Perakis, A.N., Wang, N., 2018. A real-time ship roll motion prediction using wavelet transform and variable RBF network. Ocean Eng. 160, 10–19.

Yumori, I., 1981. Real time prediction of ship response to ocean waves using time series analysis. In: OCEANS 81. IEEE, pp. 1082–1089.

Zhang, G.Y., Tan, F., Wu, Y.X., 2020. Ship motion attitude prediction based on an adaptive dynamic particle swarm optimization algorithm and bidirectional LSTM neural network (may 2020). IEEE Access (99), 1.

Zhang, C., Wei, H.K., Zhao, X., Liu, T.H., Zhang, K.J., 2016. A Gaussian process regression based hybrid approach for short-term wind speed prediction. Energy Convers. Manage. 126, 1084–1092.

Zhang, Z.D., Ye, L., Qin, H., Liu, Y.Q., Wang, C, Yu, X., Yin, X.L., Li, J., 2019. Wind speed prediction method using shared weight long short-term memory network and Gaussian process regression. Appl. Energy 247, 270–284.

Zhou, B., Shi, A.G., 2013. Empirical mode decomposition based LSSVM for ship motion prediction. In: International Symposium on Neural Networks. Springer, pp. 319–325.